International Journal of Nanomedicine

Dovepress

open access to scientific and medical research

Open Access Full Text Article

ORIGINAL RESEARCH

Novel pH-Sensitive Urushiol-Loaded Polymeric Micelles for Enhanced Anticancer Activity

This article was published in the following Dove Press journal:
International Journal of Nanomedicine

Hao Zhou*
Zhiwen Qi
Xingying Xue
Chengzhang Wang*

Institute of Chemical Industry of Forest Products, CAF; National Engineering Laboratory for Biomass Chemical Utilization; Key Laboratory of Chemical Engineering of Forest Products, National Forestry and Grassland Administration; Key Laboratory of Biomass Energy and Material, Nanjing, Jiangsu Province 210042, People's Republic of China

*These authors contributed equally to this work.

Purpose: The aim of this study was to develop a means of improving the bioavailability and anticancer activity of urushiol by developing an urushiol-loaded novel tumor-targeted micelle delivery system based on amphiphilic block copolymer poly(ethylene glycol)-b-poly-(β-amino ester) (mPEG-PBAE).

Materials and Methods: We synthesized four different mPEG-PBAE copolymers using mPEG-NH_2 with different molecular weights or hydrophobicity levels. Of these, we selected the $mPEG_{5000}$-PBAE-C_{12} polymer and used it to develop an optimized means of preparing urushiol-loaded micelles. Response surface methodology was used to optimize this formulation process. The micellar properties, including particle size, pH sensitivity, drug release dynamics, and critical micelle concentrations, were characterized. We further used the MCF-7 human breast cancer cell line to explore the cytotoxicity of these micelles in vitro and assessed their pharmacokinetics, tissue distribution, and antitumor activity in vivo.

Results: The resulting micelles had a mean particle size of 160.1 nm, a DL value of 23.45%, and an EE value of 80.68%. These micelles were found to release their contents in a pH-sensitive manner in vitro, with drug release being significantly accelerated at pH 5.0 (98.74% in 72 h) without any associated burst release. We found that urushiol-loaded micelles were significantly better at inducing MCF-7 cell cytotoxicity compared with free urushiol, with an IC_{50} of 1.21 mg/L. When these micelles were administered to tumor model animals in vivo, pharmacokinetic analysis revealed that the total AUC and MRT of these micelles were 2.28- and 2.53-fold higher than that of free urushiol, respectively. Tissue distribution analyses further revealed these micelles to mediate significantly enhanced tumor urushiol accumulation.

Conclusion: The pH-responsive urushiol-loaded micelles described in this study may be ideally suited for clinical use for the treatment of breast cancer.

Keywords: urushiol-loaded polymeric micelles, pH-sensitive, enhanced anticancer activity

Introduction

Cancer remains one of the leading causes of death globally. Chemotherapy is one of the primary treatment strategies for most cancer patients, but chemotherapeutic agents often incur significant off-target cytotoxicity and also have relatively poor bioavailability and high rates of multidrug resistance.[1] As such, the clinical utility of these drugs is often limited. A number of different targeted nanoscale drug delivery approaches have been employed in an effort to combat these limitations, including the development of nanoparticles, liposomes, polymeric micelles, and dendrimers.[2,3] Polymeric micelles are particularly advantageous for hydrophobic drug encapsulation, as they are composed of spontaneously assembling amphiphilic block copolymers that yield nanoscale particles when exposed to water.[4] As these

Correspondence: Hao Zhou; Chengzhang Wang
Institute of Chemical Industry of Forest Products, CAF, No. 16 Suojin Wucun, Nanjing, Jiangsu Province 210042, People's Republic of China
Tel +86-025-85482421; +86-025-85482471
Email zhouhaolhs@163.com; wangczlhs@sina.com

submit your manuscript | www.dovepress.com
DovePress
http://doi.org/10.2147/IJN.S250564

particles have a hydrophobic core, they can readily encapsulate hydrophobic compounds, whereas they are typically encapsulated by a hydrophilic shell composed of polyethylene glycol (PEG) or similar compounds, thus significantly improving particle systemic circulation in vivo.[5] Indeed, polymeric micelles have been found to offer advantages, including ease of production, extended circulation, and effective tumor targeting.[6] A number of drug-loaded polymeric micelles are either undergoing clinical trials or have been approved for cancer therapy, including SP1049C (doxorubicin-loaded micelles), Genexol-PM (Paclitaxel-loaded micelles), and NC-6300 (epirubicin-loaded micelles).[7]

While many advances in micellar drug delivery have been made in recent years, there are still several limitations to this technology. One of the primary limitations of this approach is the fact that drug release is generally uncontrolled following in vivo administration, resulting in low rates of drug accumulation within tumors.[8] This limitation can be overcome by developing micelles that are sensitive to tumor microenvironmental stimuli or signals, such that drug release is controlled in a targeted manner. Of the previously tested approaches, pH-sensitive polymeric micelles have been found to be promising owing to the intrinsic differences in pH levels in tumors and normal tissues.[9] The pH of the blood and the extracellular matrix is maintained at approximately 7.4, whereas low oxygen levels in the tumor microenvironment can cause the pH to fall to ~6.5. In addition, endosomes and lysosomes have lower pH values of 5.0–6.0 and 4.5–5.0, respectively.[10] By taking advantage of these pH variations, researchers have developed a number of polymeric micelles suited to releasing drugs in a controlled manner in tumor tissues, endosomes, and lysosomes. In one study, for example, Xu et al prepared a pH-responsive polymeric carrier using an amphiphilic block copolymer poly(ethylene glycol)-b-poly(2-(diisopropylamino) ethyl methacrylate) (MPEG-PPDA). Using these particles, they were able to achieve high rates of drug loading and controlled drug release in response to pH changes.[11] Similarly, Chen et al used poly(ethylene glycol)-SS-poly(2,4,6-trimethoxybenzylidene-pentaerythritolcarbonate) (PEG-SS-PTMBPEC) copolymers to prepare pH-responsive micelles that were able to readily release drugs within the tumor microenvironment, effectively killing cancer cells.[12] Xue et al also constructed a pH-sensitive amphiphilic diblock copolymer, poly (acrylic acid-b-DL-lactide) (PAAc-b-PDLLA), as a means of encapsulating and improving the controlled release of prednisone acetate.[13] Despite these advances, however, more work is needed to develop reliable and adaptable nanocarriers that can deliver drugs to tumors in a stimulus-sensitive fashion.

Urushiol is a compound that can be isolated from the sap of the lacquer tree (Rhus verniciflua Stokes, Anacardiaceae), which is grown throughout northeast Asian countries, such as China, Japan, and Korea. Urushiol is composed of o-dihydroxybenzene (catechol) bound to a 15 or 17 carbon unsaturated alkyl side chain.[14] Urushiol has been shown to be capable of potently promoting tumor cell apoptotic death and inhibiting nuclear transcription factor activity in a range of tumor types.[15] Urushiol has additionally been employed as an adjuvant treatment approach in traditional Chinese medicine (TCM) for many years. Despite its antitumor activity in vitro, urushiol has very limited solubility in water and is thus difficult to administer clinically. In addition, urushiol has poor tumor selectivity and biocompatibility, constraining its therapeutic utility and significantly increasing the risk of adverse side effects following its administration.[16] The incorporation of urushiol into pH-sensitive nanoparticles, such as polymeric micelles, has the potential to overcome these limitations by improving the stability and water solubility of this compound while allowing it to be released in a controlled manner at tumor sites in vivo. Such an approach would significantly enhance the biodistribution and pharmacokinetic profile of urushiol in a desirable manner, thus substantially increasing its clinical utility. However, no studies to date have reported the use of pH-sensitive polymeric micelles derived from amphiphilic block copolymers as a means of achieving targeted urushiol activity.

In the present study, we designed pH-responsive biodegradable polymeric micelles using poly (ethyleneglycol)-b-poly(β-amino ester) (mPEG-PBAE) amphiphilic block copolymers, and we then used these particles to efficiently deliver urushiol to tumor cells. In these micelles, mPEG functioned as the hydrophilic compound, whereas PBAE was hydrophobic and contained pH-sensitive carbamic acid ester groups. The resultant amphiphilic polymers were found to readily self-assemble into micelles when exposed to an aqueous environment. Importantly, urushiol, which contains a hydrophobic region as well as a pair of hydroxyl groups, was readily encapsulated in the core of these micelles through both hydrophobic and hydrogen bonding interactions. A membrane dialysis approach was used to prepare these urushiol-loaded polymeric micelles, with a star point design-based RSM approach used to optimize the

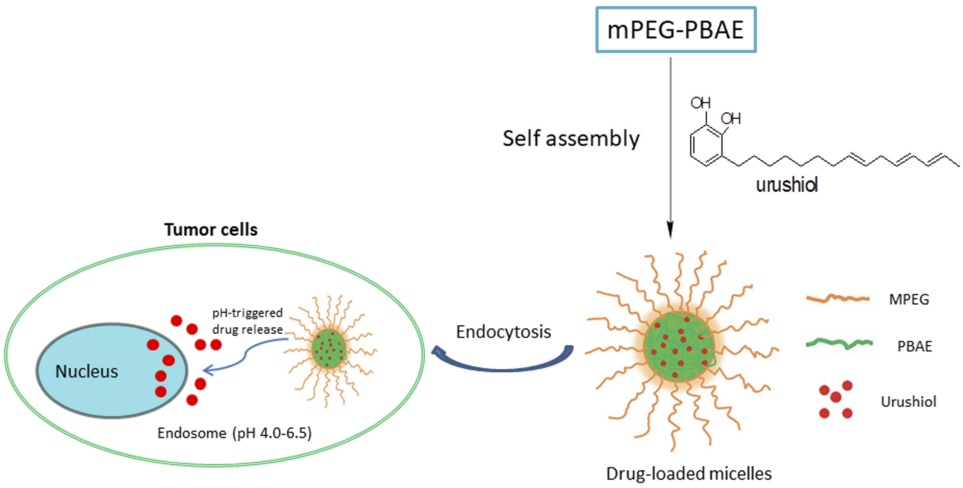

Figure 1 Schematic illustration of forming pH-responsive urushiol-loaded polymeric micelles and the pH-triggered drug-release mechanism.
Abbreviation: mPEG-PBAE, poly(ethylene glycol)-b-poly-(β-amino ester).

formulation methodology described herein. After formulation was complete, we fully characterized the micellar properties, including particle size, pH sensitivity, drug-release dynamics, and critical micelle concentrations. We further used the MCF-7 human breast cancer cell line to explore the cytotoxicity of these micelles in vitro, and we assessed their pharmacokinetics, tissue distribution, and antitumor activity in vivo. We hypothesized that these urushiol-loaded polymeric micelles would improve the antitumor efficacy of urushiol by facilitating pH-sensitive targeted drug release (Figure 1).

Materials and Methods

Materials

Methoxy poly(ethylene glycol)-amino (mPEG-NH_2, Mw=2000, 5000 Da), dodecylamine, tetradecylamine, 5-amino-1-pentanol, 1,3-diaminopentane (DAMP), and 1,4-butanediol diacrylate (BUDA) were from Shanghai Aladdin Bio-technique Co. Ltd. (Shanghai, China). N, N-dimethylformamide (DMF), tetrahydrofuran (THF), pyrene, and acetone were from Sinopharm Chemical Reagent Co. Ltd. (Shanghai, China). DMEM, 3-(4,5-dimethylthiazol-2-yl)-2,5-diphenyltetrazolium bromide (MTT), fetal bovine serum (FBS), trypsin–EDTA, and penicillin-streptomycin were from Nanjing Norman Bio-technique Co. Ltd. (Nanjing, China). Urushiol was isolated internally and was found to be pure via HPLC (≥95%). MCF-7 cells were from the cell center of the Chinese Academy of Medical Sciences. All other chemicals were of analytical grade and were used as provided.

mPEG-PBAE Synthesis

We synthesized the mPEG-PBAE copolymer using a slightly modified version of a previous protocol.[17] Briefly, anhydrous DMSO was used to dissolve mPEG-NH_2 (Mw = 2000 or 5000 Da)(0.08 equiv), hydrophobic amino (dodecylamine or tetradecylamine)(0.7 equiv), 5-amino-1-pentanol (0.3 equiv), and 1,4-butanediol diacrylate (1.2 equiv) at 0.2 mg/mL. The mixture was stirred for 24 h at 60°C, after which we added 1, 3-diaminopentane (1.4 equiv) and stirred the mixture for an additional 24 h at 60 °C. Next, 20 mL dichloromethane was added to the solution, and deionized water was used to wash the solution three times prior to overnight separation and drying of the organic solution using anhydrous magnesium sulfate. The organic phase was next filtered, concentrated using a rotating evaporator under vacuum conditions, and dried for 24 h at 40 °C under vacuum conditions, yielding the pH-sensitive mPEG-PBAE copolymer.

mPEG-PBAE Characterization

Nuclear Magnetic Resonance Spectroscopy (NMR)

^{1}H NMR was used to characterize the chemical structures of these mPEG-PBAE copolymers.[18] A Bruker AVANCE 500 spectrometer (Bruker, Switzerland) was used to characterize the ^{1}H-NMR of mPEG-PBAE using DMSO-d_6 at a 10 mg/mL polymer concentration. Measurements were conducted at 300 K using the pulsed accumulation of 64 scans and an LB parameter of 0.30 Hz. Tetramethylsilane was employed for internal standardization.

FT-IR Analysis

A Nicolet 380 spectrometer (Thermo Scientific, WI, USA) was used to assess the FT-IR spectra of polymers from 4000–600 cm^{-1} (32–64 scans; 4 cm^{-1} resolution) at room temperature. For this analysis, samples were combined with potassium bromide and punched into tablets via hydraulic pressing. The OMNIC 8 spectrum software (Thermo Scientific, Waltham, USA) was used for analysis.

Gel Permeation Chromatography (GPC)

GPC was conducted to assess the copolymer molecular weight (M_W) and polydispersity index (PDI) values using a Waters 2695 pump and a Styragel HT4DMF column (Waters, MA, USA). Copolymers were dissolved at 3–4 mg/mL in tetrahydrofuran and analyzed via injection at a 1 mL/min flow rate at 25°C, with THF serving as an eluent. PEG standards were used for M_W calibration.

Critical Micelle Concentration (CMC) Measurement

We measured the CMC of our copolymers in aqueous solution by using pyrene as a fluorescent probe in a fluorescence spectroscopy analysis, as reported previously.[19] Briefly, we prepared a stock solution of 25 mg pyrene in acetone and then serially diluted this solution to a final concentration of 2×10^{-4} mol/L. A 100 μL volume of this solution was then added to individual 10 mL volumetric flasks, and the acetone diluent was dissolved under mild heat. A 10 mL volume of mPEG-PBAE (1.22×10^{-4} - 2.0 mg/mL) in deionized (DI) water was then added to each tube. The pyrene concentrations were then adjusted to 2×10^{-4} mol/L, and samples were sonicated in a water bath for 30 minutes prior to equilibration at room temperature overnight. A fluorescence spectrophotometer (Shimizu, Tokyo, Japan) was then used to analyze the fluorescence of individual samples, with 340 nm used as an excitation wavelength for pyrene and 373 and 383 nm serving as emission wavelengths corresponding to the first and third vibrational peaks of pyrene, respectively. We then blotted the intensity ratios of the first to the third peaks (I_1, I_3) against polymer concentration on a logarithmic scale. Tangents were then drawn, with the CMC being determined based upon the intersection of these tangents.

Urushiol-Loaded Micelle Preparation

A membrane dialysis approach was employed for the preparation of urushiol-loaded polymeric micelles. Briefly, we combined 15 mg urushiol and 50 mg mPEG-PBAE copolymer in a 10 mL volume of DMF. The mixture was sonicated for 30 minutes at room temperature, after which it was dialyzed at room temperature against dH_2O for 24 h with a dialysis membrane (MWCO: 3.0 kDa), with the distilled water being refreshed on an hourly basis. The micelle-containing solution was then spun for 10 minutes at 1000 rpm and filtered through a 0.45 μm membrane to yield drug-loaded micelles. These micelles were then lyophilized and stored at 4°C prior to analysis. In addition, blank polymeric micelles were prepared via the same general approach, omitting the urushiol and sonicating samples for 10 minutes prior to dialysis for 24 h.

Optimization of Drug-Loaded Micelle Formulation

Star point design response surface methodology (RSM) was employed to determine the optimal formulation strategy for urushiol-loaded polymeric micelles. This approach sought to maximize drug loading content (DL%) and drug encapsulation efficiency (EE%) in the resultant micelles. Based on preliminary findings, we fixed copolymer levels at 50 mg and varied the amounts of urushiol (A, in mg) and DMF (B, in mL), as these were found to significantly affect DL and EE. For details regarding the amounts of these compounds used in this RSM approach, see Table 1. The final factorial design of this study included 8 factorial points and 5 central points, and Design-Expert software (v8.05) was used for the analysis.

Urushiol-Loaded Polymeric Micelle Physicochemical Characterization

Size Distribution and Zeta-Potential Quantification

Dynamic light scattering (DLS) and laser Doppler electrophoresis using Zetasizer Nano ZS90 (Malvern Instruments Ltd., Worcestershire, UK) with a He-Ne laser (633 nm) and 90° collecting optics were used to assess the size distributions and zeta potential values for these micelles (in nm and mV, respectively). Temperatures were maintained at 25°C during analysis, and triplicate analyses were performed.

Transmission Electron Microscopy (TEM)

A JEOL JEM-2000 (Tokyo, Japan) instrument with a Gatan 94 Ultrascan 1k charge-coupled camera was used for the morphological analyses of micelles. Briefly, individual drops of a 2 mg/mL urushiol-loaded polymeric micelle solution were added to a carbon-coated copper grid. Samples were then allowed to dry at room temperature prior to TEM analysis at a 200 kV accelerating voltage.

Table 1 Theoretical Composition, Yield and Molecular Weight of mPEG-PBAE Copolymers

Sample	Feed Ratio/moL					Yield/%	Molecular Weight (g/moL)		
	$mPEG-NH_2$	BUDA	LA	HA	DAMP		Mw	Mn	PDI
$mPEG_{2000}$-PBAE-C_{12}	0.08	1.2	0.7	0.3	1.4	81.3	7395	5438	1.36
$mPEG_{2000}$-PBAE-C_{14}	0.08	1.2	0.7	0.3	1.4	80.4	8491	6336	1.34
$mPEG_{5000}$-PBAE-C_{12}	0.08	1.2	0.7	0.3	1.4	86.5	10,395	8250	1.26
$mPEG_{5000}$-PBAE-C_{14}	0.08	1.2	0.7	0.3	1.4	78.6	11,348	8866	1.28

Abbreviations: mPEG-PBAE, poly(ethylene glycol)-b-poly-(β-amino ester); BUDA, 1,4-butanediol diacrylate; LA, lipophilic amine; HA, hydrophilic amine; DAMP, 1,3-diaminopentane; Mw, weight average molecular weight; Mn, number average molecular weight; PDI, polydispersity index.

Quantification of Drug Loading and Encapsulation Efficiency

High-performance liquid chromatography (HPLC) was used to measure DL in these polymeric micelles. Briefly, 10 mL of methanol was used to dissolve 0.1 g of lyophilized urushiol-loaded micelles. Samples were stirred for 1 h, after which they were passed through a 0.45 μm nylon filter, and 20 μL of the filtered solution was directly injected into an HPLC system (LC-20A HPLC Pump, Shimadzu, Japan) equipped with an Agilent ZORBAX SB-C18 column (4.6 mm × 150 mm, 2.1 μm particle size). The mobile phase for this analysis was a 25:5 mixture of methanol and water; the column was warmed to 30°C, while the flow rate was set to 0.3 mL/min. A UV detector recorded the resultant signals at 277 nm, with urushiol concentrations between 0.02 and 0.16 mg/mL determined using a calibration line. Using this approach, the R^2-value of the peak area versus urushiol concentration was no lower than 0.998. Drug loading content (Eq. (1)) and encapsulation efficiency (Eq. (2)) were calculated as follows:

$$\text{Drug loading content (DL\%)} = \frac{wt\ of\ the\ urushiol\ in\ micelles}{wt\ of\ the\ micelles} \times 100\% \quad (1)$$

$$\text{Drug encapsulation efficiency (EE\%)} = \frac{wt\ of\ the\ urushiol\ in\ micelles}{wt\ of\ the\ feeding\ urushiol} \times 100\% \quad (2)$$

In vitro Stability

A serum protein adsorption assay was used to estimate the stability of urushiol-loaded micelles. Briefly, 18 mL of urushiol-loaded micelle solution (1 mg/mL) was mixed with 2 mL of FBS and then incubated at 37 °C for 24 h. Particle diameter and PDI were measured after 0, 4 and 24 h. At each time point, 5 mL of the solution was diluted with fresh filtrated purified water and analyzed with the DLS.

Assessment of Micelle pH Sensitivity

In an effort to simulate the pH conditions found in vivo, micelles were resuspended in PBS solutions with a pH of 5.0, 6.5, or 7.4. Samples were then shaken at 120 rpm at 37°C, and samples were collected at appropriate time points for DLS-mediated analysis of particle size.

In vitro Drug-Release Profile Analysis

A dialysis-bag diffusion approach was used to analyze the dynamics of urushiol release from polymeric micelles in vitro. Briefly, urushiol-loaded polymeric micelles (200 mg) were added to 50 mL of PBS at defined pH values, and samples were shaken gently at 37°C. Next, 5 mL aliquots of a 4 mg/mL micelle solution were added to three separate dialysis bags, which were then immersed in 50 mL of PBS at a pH of 5.0, 6.5, or 7.4. Tubes were shaken at 37°C, and a 10 mL aliquot of PBS from each tube was regularly withdrawn and replaced with an equivalent volume of fresh PBS. Urushiol release was then quantified via HPLC as above.

In vitro Cytotoxicity Assay

An MTT assay was used to analyze the cytotoxic properties of urushiol and/or polymeric micelles in this study.[20] Briefly, MCF-7 cells were cultured in RPMI-1640 containing 10% FBS and penicillin/streptomycin at 37°C and 5% CO_2. Cells were passaged at regular time points with trypsin/EDTA prior to experimental utilization. For the MTT assay, these cells were plated at 3×10^4 cells/well in 96-well plates and were allowed to grow until 75% confluent, at which time blank polymeric micelles (10–500 mg/L), urushiol-loaded polymeric micelles (containing 0.001–20 mg/L urushiol) or free urushiol (0.001–20 mg/L) were added to appropriate wells. Plates

were then incubated for 48 h, after which 20 μL of MTT solution (5 mg/mL in 0.02 M phosphate buffer) was added per well, and cells were incubated for an additional 4 h. Medium was then removed from these plates, and 150 μL of DMSO was added per well to facilitate formazan crystal dissolution. A microplate reader (Stat Fax-2100; Awareness Technology, Inc., FL, USA) was then used to quantify the absorbance at 570 nm. Untreated cells and blank media were used as controls.

In vivo Pharmacokinetic Analyses

Male Wistar rats (250 ± 20 g) were used for pharmacokinetic analyses. Briefly, animals were fasted overnight with free access to water and were then administered the indicated doses of appropriate formulations. Free urushiol was dissolved in a solvent of DMSO/PEG_{400}=2/8. Animals were randomly separated into 3 groups (n=8/group) and intravenously administered a solution of either free urushiol (20 mg/kg) or urushiol-loaded polymeric micelles (equivalent of 20 mg/kg urushiol dose). Blood was collected into heparinized tubes from the subclavian vein of these rats at appropriate time points (0.25, 0.5, 1, 2, 4, 6, 8, 12, 24, 48 h), and this blood was immediately spun for 15 minutes at 4000 rpm. The plasma-containing supernatant was then collected, and methanol was used to extract the urushiol. Methanol was then evaporated under nitrogen flow, and the residue was dissolved in fresh methanol and subjected to HPLC analysis. Pharmacokinetics were measured using a noncompartmental model with Drug and Statistics (DAS) software (v2.1.1, Mathematical Pharmacology Professional Committee, China).

In vivo Antitumor Activity and Tissue Distribution Assays

For in vivo efficacy experiments, MCF-7 cells were subcutaneously implanted into female Kunming mice (18–22 g; 1×10^7 cells/mouse). Tumors were allowed to grow to between 100 and 200 mm^3 in size, at which time the mice were randomized into three treatment groups (n=12/group): normal saline (NS), free urushiol (10 mg/kg), and urushiol-loaded polymeric micelles (10 mg/kg urushiol equivalent dose). Animals received injections of the indicated treatments through the tail vein once every other day for 14 days total (200 uL/injection). Tumor volumes and body weight in these mice were then monitored over a 20-day period. In addition, tumor volume was calculated following the measurement of tumor length and width with digital calipers as follows: ($width^2$ ×length)/2. On day 20 post-injection, animals were euthanized and tumors collected, at which time the inhibition of tumor growth for the indicated treatments was calculated. In addition, tissue distribution assays were conducted by sacrificing three randomly selected mice in the free urushiol and urushiol-loaded polymeric micelle groups at 5 min, 30 min, 1 h, 2 h, 4 h, 8 h, and 12 h following administration of the indicated treatments. Major organs (tumor, heart, liver, spleen, lungs, and kidneys) were collected from these animals, weighed, and homogenized in normal saline. The urushiol content was then extracted and quantified.

Results and Discussion

Amphiphilic Block Copolymer Synthesis and Characterization

A one-pot method was used to synthesize mPEG-PBAE amphiphilic block copolymers (Figure 2). Initially, mPEG-NH_2, a hydrophobic amine monomer, 5-amino-1-pentanol, and excess 1,4-butanediol diacrylate were combined for 24 h in DMSO, yielding a polymer containing acrylate. Next, we added 1,3-pentanediamine, which, through a Michael addition reaction with acrylate, yielded an amphiphilic mPEG-PBAE copolymer with a terminal amino group. This copolymer was composed of a hydrophilic mPEG chain together with a pH-sensitive hydrophobic PBAE chain that was sufficiently long to ensure micelle stability and to thereby facilitate controlled release of urushiol. In acidic conditions, this PBAE chain can become hydrophilic, thus allowing for pH-mediated release of encapsulated cargo. We initially synthesized four different polymers using mPEG-NH_2 of different molecular weights (M_W = 2000 or 5000 Da) and different hydrophobic amino sources (dodecylamine or tetradecylamine), yielding the following polymers: $mPEG_{2000}$-PBAE-C_{12}, $mPEG_{2000}$-PBAE-C_{14}, $mPEG_{5000}$-PBAE-C_{12} and $mPEG_{5000}$-PBAE-C_{14}.

These four polymers were successfully synthesized, as validated by their respective ^{1}H NMR (Figure 3) and FTIR spectra (Figure 4). In the corresponding FT-IR spectra, a characteristic peak consistent with an ether bond was evident at 1104–1109 cm^{-1}, with additional peaks at 1730–1732 cm^{-1} further confirming the presence of an ester bond-containing block copolymer. In the ^{1}H NMR spectra, we were able to observe peaks at 3.98, 3.99, 1.60, 1.59, and 1.17–1.22 ppm that corresponded to the methylene protons of -$COOCH_2$- and -CH_2CH_2- in the PBAE segment, while peaks at 2.30–2.63 ppm corresponded to -CH_2- and -CH- protons, which were

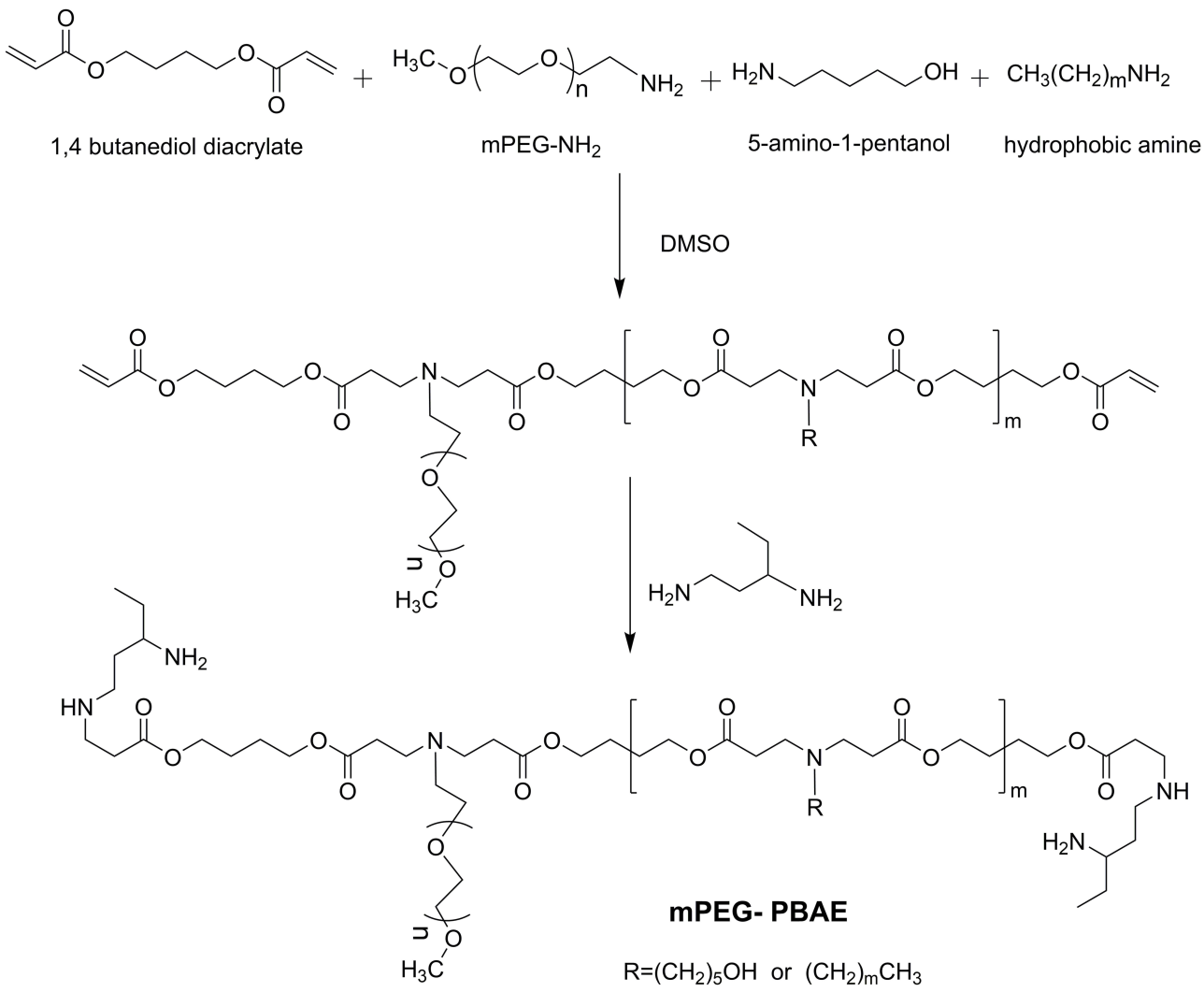

Figure 2 Synthesis route of pH-responsive mPEG-PBAE block copolymers.
Abbreviations: mPEG-PBAE, poly(ethylene glycol)-b-poly-(β-amino ester); DMSO, dimethyl sulphoxide.

connected to -NH-, –N-, and NH_2- groups. Furthermore, the peaks that were evident at 3.30 and 3.50 ppm were consistent with the methyl and methylene protons of -OCH_2CH_2- and -OCH_3 groups in the mPEG segment, while the 0.78–0.84 ppm peaks were consistent with -CH_2CH_3 methyl protons located at the end of the chain. Importantly, the peaks at 5.5–6.0 ppm were not evident in the final polymers, confirming the successful reaction of acrylate with 1, 3-pentanediamine at the end of the polymer. These findings confirmed that all four isoforms of mPEG-PBAE copolymer had been prepared successfully.

We next employed GPC to analyze the M_W and distribution of these four polymers (Table 1). The $mPEG_{2000}$-PBAE-C_{12}, $mPEG_{2000}$-PBAE-C_{14}, $mPEG_{5000}$-PBAE-C_{12}, and $mPEG_{5000}$-PBAE-C_{14} polymers had measured M_W values of 7395, 8491, 10,395, and 11,348 Da, respectively. In addition, each of these polymers had a polydispersity index (PDI) of < 1.4, consistent with a relatively narrow M_W distribution for each of these copolymers. We achieved satisfactory yields for all of these polymers, with the yield of $mPEG_{5000}$-PBAE-C_{12} being the highest (86.5%). Copolymer stability and aggregation can be analyzed by measuring the CMC value,[21] and a pyrene fluorescence probe approach was used for measurements in the present study. We found that the $mPEG_{2000}$-PBAE-C_{12}, $mPEG_{2000}$-PBAE-C_{14}, $mPEG_{5000}$-PBAE-C_{12}, and $mPEG_{5000}$-PBAE-C_{14} polymers had CMC values of 37.58, 31.70, 18.25, and 27.61 mg/L, respectively (Figure 5). Lower CMC values indicate that copolymers are able to form micelles at lower concentrations and that the resultant micelles are stable in solution. We found that the $mPEG_{5000}$ copolymers had lower CMC values relative to the $mPEG_{2000}$ copolymers, suggesting that $mPEG_{5000}$ may form a thicker hydrophobic shell than $mPEG_{2000}$, yielding

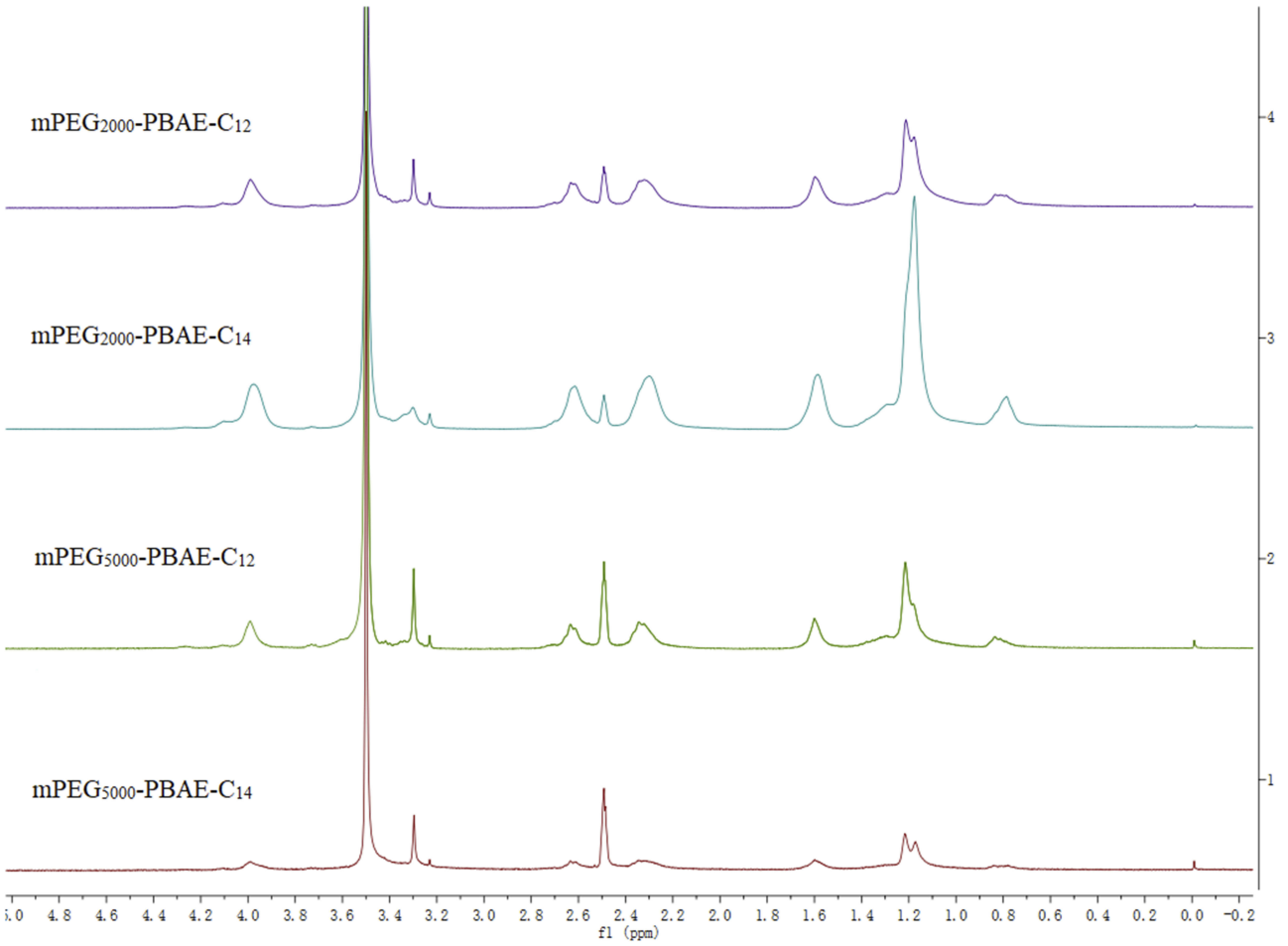

Figure 3 ^{1}H NMR spectra of four kinds of mPEG-PBAE copolymers.
Abbreviations: mPEG-PBAE, poly(ethylene glycol)-b-poly-(β-amino ester); NMR, nuclear magnetic resonance.

a polymer with a longer hydrophobic block that can more readily undergo self-assembly into micelles in solution.

We found that these mPEG-PBAE copolymers were readily able to self-assemble into micelles. The fate of such micelles following in vivo administration is profoundly influenced by the size of these particles, with a size of < 200 nm being preferable for the passive targeting of micelles to tumors via the EPR effect.[22] We found that the $mPEG_{2000}$-PBAE-C_{12}, $mPEG_{2000}$-PBAE-C_{14}, $mPEG_{5000}$-PBAE-C_{12}, and $mPEG_{5000}$-PBAE-C_{14} micelles had average particle sizes of 159.1, 204.6, 149.1 and 237.5 nm, respectively, with corresponding zeta-potential values of 24.9, 17.7, 32.8, and 16.9 mV (Table 2). This indicated that the $mPEG_{5000}$-PBAE-C_{12} micelles exhibit both the highest measured zeta potential and a suitable particle size. Zeta potential is associated with the stability and dispersion of micelles, with higher values corresponding to a greater repulsive force between particles that can drive better particle dispersion, reducing condensation and improving system stability.[21] We additionally measured the drug loading capacity (DL%) of these four copolymers, yielding respective DL values of 13.92, 15.25, 23.92, and 21.28%. Micelles derived from polymers incorporating $mPEG_{5000}$ exhibited markedly higher DL values relative to those of micelles derived from $mPEG_{2000}$. This is likely attributable to the higher molecular weight of $mPEG_{5000}$, as this would yield a larger lipophilic nucleus capable of additional drug loading.

Urushiol-Loaded Polymeric Micelle Formulation Optimization

In light of the above characterization results, we selected the $mPEG_{5000}$-PBAE-C_{12} polymer for further use in the optimization of the loading conditions of urushiol in an effort to yield stable and efficacious drug-loaded micelles.

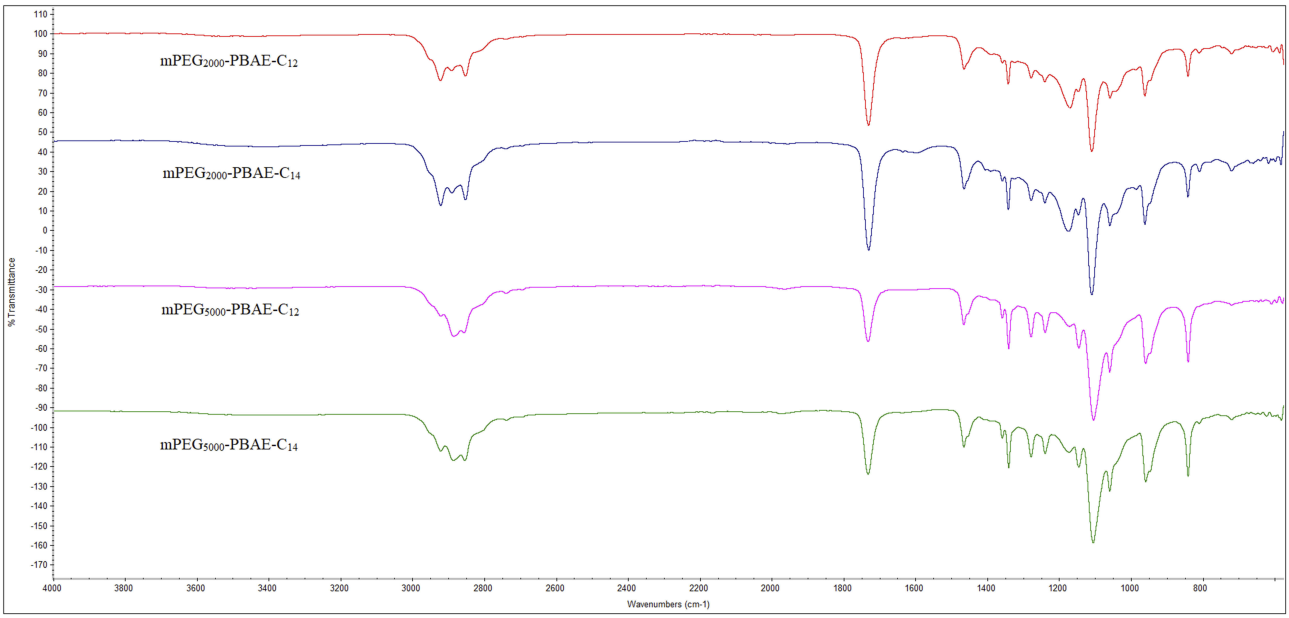

Figure 4 FT-IR spectra of four kinds of mPEG-PBAE copolymers.
Abbreviations: mPEG-PBAE, poly(ethylene glycol)-b-poly-(β-amino ester); FT-IR, Fourier transform-infrared spectroscopy.

We selected a fixed polymer amount (50 mg) in light of the above studies, and we varied the urushiol and solvent dosages (A and B, in mg and mL, respectively) to maximize the DL (Y_1) and EE (Y_2) of the resultant drug-loaded micelles. The interactions between these two independent variables were assessed at three levels (low, basal, high; coded as 0 and ±1) using a starting point of ±1.414 for ±α in the RCCD pattern. We then conducted 13 experiments, with the resultant responses being compiled and analyzed (Tables 3 and 4). The DL and EE values were compared with Design Expert Software. An ANOVA assessment of the second-order polynomial model of the relationship between these variables yielded DL% and EE% F-values of 92.25 and 137.4, respectively, with P-values < 0.0001 consistent with a significant effect (Table 5). Furthermore, these two variables yielded R^2 values of 0.9851 and 0.9899, respectively, while their respective Adeq Precision ratios were 27.668 and 33.05, indicating a good match between the predicted and experimental values. As such, we were able to use the model to simulate and optimize urushiol-loaded polymeric micelle preparations. We found that urushiol dosage, squared urushiol dosage, and squared solvent dosage all significantly impacted the resultant DL% and EE% values of our drug-loaded micelles ($P < 0.05$; Table 5). The following second-order polynomial models were ultimately obtained, with urushiol and solvent dosages represented as A and B, respectively: $Y_1(DL/\%) = -9.179+2.821\times A + 1.436\times B-0.077\times A^2-0.074\times B^2+0.0052\times A\times B$; $Y_2(EE/\%) =59.589+1.316\times A+5.074\times B-0.109\times A^2-0.253\times B^2 +0.0021\times A\times B$.

We additionally generated 3D response surface plots corresponding to both the DL and EE values for prepared drug-loaded micelles to directly visualize interactions between variables and responses in this experimental system (Figure 6). We found that, when the solvent dosage was fixed, DL% values first increased with rising urushiol doses before later declining, suggesting that urushiol concentrations eventually reached saturating levels, after which the drug was no longer able to enter the micelles, thus decreasing the efficiency of drug loading. Similarly, at a fixed solvent dosage, we found that DL% initially rose with increasing solvent dose before later declining, likely because the dispersion of micelles in solution increases significantly at high solvent concentrations, thus decreasing the rate of urushiol loading into these micelles. We also found that EE% rose significantly with increasing solvent dosage before later declining when the amount of urushiol was fixed, and EE% also rose significantly in the context of a fixed solvent dosage when urushiol amounts rose from 3.0–15.0 mg before declining significantly at urushiol concentrations > 15.0 mg. This suggests that urushiol saturation of the solution may also result in urushiol precipitation, thus reducing the EE% for the resultant micelles.[23]

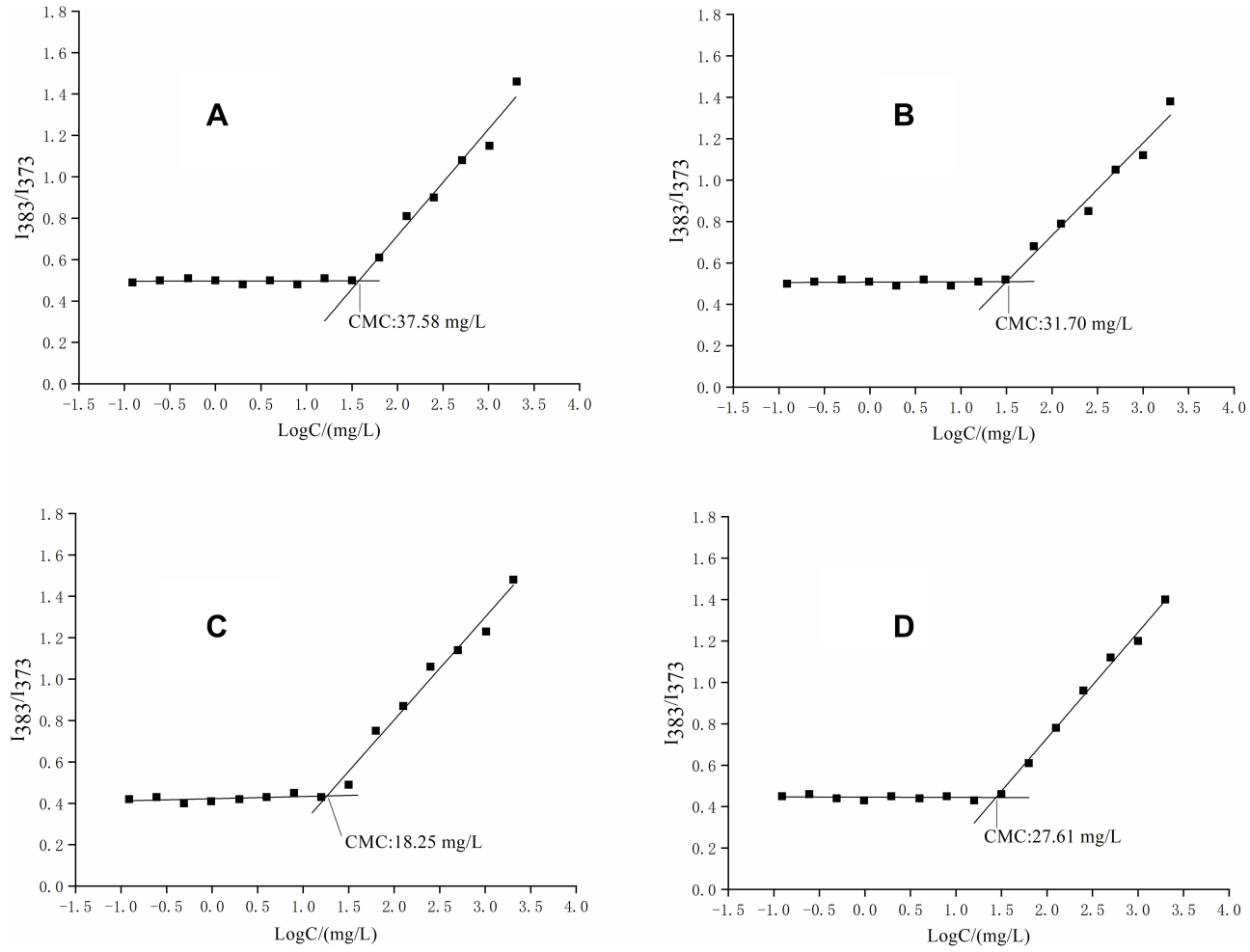

Figure 5 CMC of mPEG-PBAE micelles, derived from the plot of I_{373}/I_{383} ratio vs copolymer concentration.
Notes: (**A**) $mPEG_{2000}$-PBAE-C_{12}, (**B**) $mPEG_{2000}$-PBAE-C_{14}, (**C**) $mPEG_{5000}$-PBAE-C_{12}, (**D**) $mPEG_{5000}$-PBAE-C_{14}.
Abbreviations: CMC, critical micelle concentration; mPEG-PBAE, poly(ethylene glycol)-b-poly-(β-amino ester).

Finally, we employed the numerical optimization tools in Design Expert software, which predicted that the optimal 23.51% DL and 80.55% EE could be achieved with 10 mL of solvent and 15 mg of urushiol. To test the validity of this model, we prepared urushiol-loaded polymeric micelles based on these predicted conditions, and we compared the predicted and experimentally derived values for the resultant particles (Table 6). This analytical approach confirmed that we were able to achieve maximal DL (23.45%) and EE (80.68%)

Table 2 Particle Size, Zeta Potential and DL of mPEG-PBAE Copolymer Micelles

Sample	Particle Size (nm)	Zeta Potential (mV)	DL (%)
$mPEG_{2000}$-PBAE-C_{12}	159.1±2.2	24.9±0.65	13.92 ±0.15
$mPEG_{2000}$-PBAE-C_{14}	204.6 ± 4.3	17.7±0.41	15.25 ±0.18
$mPEG_{5000}$-PBAE-C_{12}	149.1±2.1	32.8±0.86	23.92 ±0.36
$mPEG_{5000}$-PBAE-C_{14}	237.5±5.4	16.9±0.38	21.28 ±0.20

Note: Data presented as mean ± standard deviation (n=3).
Abbreviations: mPEG-PBAE, poly(ethylene glycol)-b-poly-(β-amino ester); DL, drug loading.

Table 3 Factors and Responses in Star Point-Based RSM Design

Variables	Levels					
	Symbols	−1.414	−1	0	1	1.414
Urushiol dosage/mg	A	3	6.513	15	23.487	27
Solvent dosage/mL	B	2	4.342	10	15.658	18

Abbreviation:RSM, response surface methodology.

Table 4 Scheme of Star Point-Based RSM Design with the Results of Responses on Two Independent Factors

No.	Independent Variables				Dependent Variables	
	Levels	Urushiol Dosage (A)/mg	Levels	Solvent Dosage (B)/mL	DL/ %	EE/ %
1	−1	6.513	−1	4.342	11.15	83.60
2	1	23.487	−1	4.342	18.85	48.13
3	−1	6.513	1	15.658	10.92	81.83
4	1	23.487	1	15.658	19.62	46.77
5	−1.414	3	0	10	5.21	85.83
6	1.414	27	0	10	20.46	42.89
7	0	15	−1.414	2	18.9	62.05
8	0	15	1.414	18	19.49	65.67
9	0	15	0	10	22.87	79.23
10	0	15	0	10	22.96	79.53
11	0	15	0	10	23.95	80.83
12	0	15	0	10	23.54	80.47
13	0	15	0	10	24.21	82.70

Abbreviations: DL, drug loading; EE, encapsulation efficiency; RSM, response surface methodology.

under these optimized conditions, with actual values being within 1% of the predicted values. This finding was consistent across multiple batches of micelles, confirming the validity and reliability of this micelle preparation strategy.

Urushiol-Loaded mPEG-PBAE Micelle Characterization

Using a dialysis-based approach, we prepared urushiol-loaded $mPEG_{5000}$-PBAE-C_{12} micelles using the optimized conditions discussed above before characterizing these particles via DLS and TEM to establish their size distribution and morphological characteristics. The resultant micelles were found to be 160.1 nm in diameter and to have a narrow unimodal diameter distribution (Figure 7A). The size of these drug-loaded micelles was thus only slightly larger than that of the blank micelles, with this change likely being attributable to changes in the hydrophobic bond force with the micellar core upon urushiol loading. This finding further confirmed that successful drug loading had been achieved. We also found that these particles had a relatively high zeta potential (33.40 mV), consistent with their satisfactory stability following drug-loading. A TEM analysis revealed that these micelles were uniform spheroid particles that were monodispersed (Figure 7B). TEM-based size estimates were in line with the results of the above particle size analysis, further confirming that these micelles can remain stable and readily dispersed in an aqueous solution. These properties also make these particles ideal for the penetration of tumors via the enhanced permeability and retention effect (EPR).[24]

In vitro Stability Assay

Before the release experiments, urushiol-loaded micelles were incubated in the presence of FBS, and in vitro stability was determined. Because positively charged drug carriers can bind to negatively charged serum protein, they tend to accumulate in the blood and cannot effectively reach the tumor. Therefore, we used serum protein to verify the stability of urushiol-loaded micelles in the blood. The change of particle size and PDI in 10% FBS within 24 hours was determined by DLS (Figure 8). There was no significant change in particle size or PDI observed for urushiol-loaded micelles; in 24 hours, the average particle size changed from 160.5 to 163.3, and the PDI changed from 0.138 to 0.141, indicating no aggregation. The urushiol-loaded micelles possess good antisera protein adsorption ability and can be stable in serum. Their anti-protein adsorption mechanism is related to hydration, as the PEG chain of

Table 5 Analysis of Variance (ANOVA) for Response Surface Quadratic Model for DL% (Y_1) and EE% (Y_2)

Source	Sum of Squares		df	Mean Square		F value		P-value(Prob>F)*	
	Y1	Y2		Y1	Y2	Y1	Y2	Y1	Y2
Model	414.66	2937.66	5	82.93	587.53	92.25	137.54	<0.0001	<0.0001
A- urushiol dosage	180.18	2153.53	1	180.18	2153.53	200.43	504.13	<0.0001	<0.0001
B- solvent dosage	0.24	0.49	1	0.24	0.49	0.26	0.12	0.6241	0.7436
AB	0.25	0.042	1	0.25	0.042	0.28	0.0098	0.6143	0.9238
A^2	214.70	428.99	1	214.70	428.99	238.82	100.43	<0.0001	<0.0001
B^2	39.26	456.74	1	39.26	456.74	43.67	106.92	0.0003	<0.0001
Pure error	1.40	7.49	4	0.35	1.87				
Cor total	420.95	2967.56	12						

Notes: *Values of "Prob > F" <0.0500 indicate model terms are significant.
Abbreviations: DL, drug loading; EE, encapsulation efficiency.

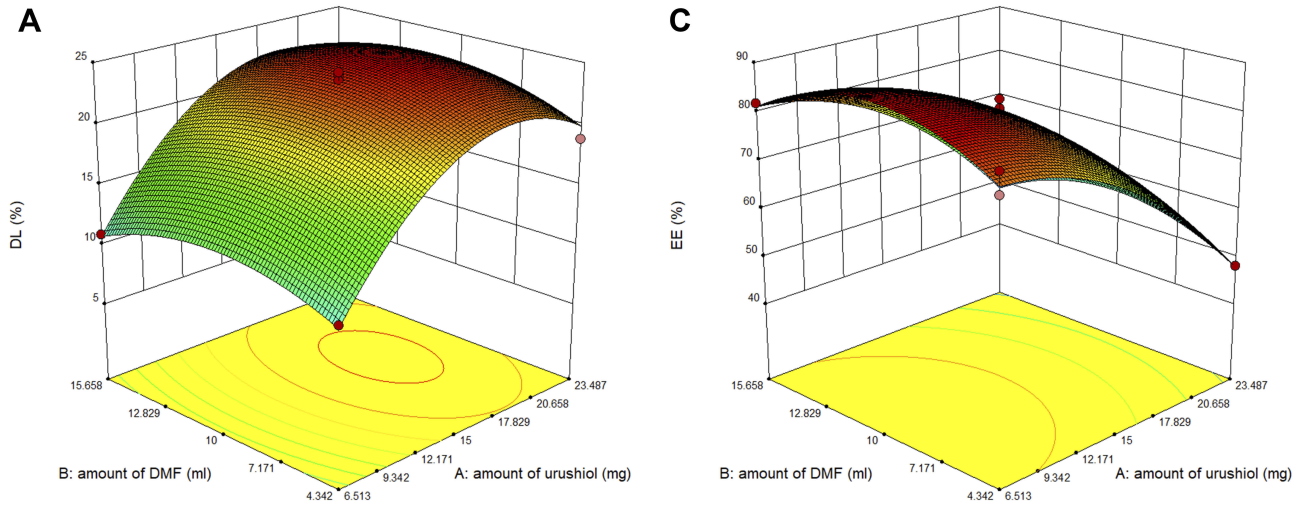

Figure 6 Predicted three-dimensional (3D) response surface model showing the variation DL% (**A**) and EE% (**B**) with changes in independent variables of urushiol dosage and solvent dosage.
Abbreviations: DL, drug loading; EE, encapsulation efficiency; DMF, N, N-dimethylformamide.

amphiphilic copolymers has strong hydrophilicity, which can greatly improve the water absorption ability of the polymer and minimize the adsorption of serum protein. The binding of water on the surface of the micelles is the main reason preventing the material from absorbing protein.[25]

Assessment of in vitro Micellar Urushiol Release in Response to pH Changes

We next sought to confirm that our urushiol-loaded micelles were able to release urushiol in a controlled manner in response to pH changes. To that end, we suspended these micelles in aqueous solutions with a range of pH values (5.0, 6.5 or 7.4) and then examined the size of the particles via DLS. We found that, following a 24-h incubation in PBS solution with a pH of 7.4, negligible changes in particle size were evident, suggesting that these particles are extremely stable at a normal physiological pH (Figure 9A). However, when the pH was lowered to 5.0, we found that the particles grew in size from 160 nm to 305 nm within 4 h before eventually growing to 625 nm after 24 h. At the higher pH of 6.5, particle size instead rose to 292 nm at 24 h. These significant changes in particle size under acidic conditions suggest that these urushiol-loaded micelles underwent dissociation as a result of the proton sponge effect. The primary, secondary, and tertiary amine groups found within the polymer are able to absorb protons in an acidic solution. This, in turn, leads to an increase in the positive charge of the polymer, causing an increase in electrostatic repulsive forces that lead to particle expansion. Furthermore, hydrogen binding in this context may have additionally led to micelle agglomeration, thus further increasing the observed particle size.[26] As the swelling of these micelles was more significant at a pH of 5.0 relative to a pH of 6.5, these micelles likely expand and aggregate more readily in highly acidic environments. We did observe a slight decrease in micelle size following a 1-h incubation at pH 5.0, which may be attributable to the hydrolysis of ester bonds within the polymer. Such bond hydrolysis would have further disrupted the integrity of the polymer and the structural integrity of these micelles, leading to a reduction in particle size but increasing the ability of these particles to aggregate and form secondary micellar structures via self-assembly in solution. Based on these findings, we can conclude that urushiol-loaded micelles are very stable when exposed to a normal physiological pH, whereas

Table 6 Comparison of the Experimental and Predicted Values of Urushiol-Loaded Micelle Prepared Under the Predicted Optimum Conditions

Response	Predicted Value	Experimental Value	% bias
Y1 = DL (%)	23.51	23.45 ±0.68	0.26
Y2 = EE (%)	80.55	80.68 ±2.54	−0.16

Note: Data presented as mean ± standard deviation (n=3).
Abbreviations: DL, drug loading; EE, encapsulation efficiency.

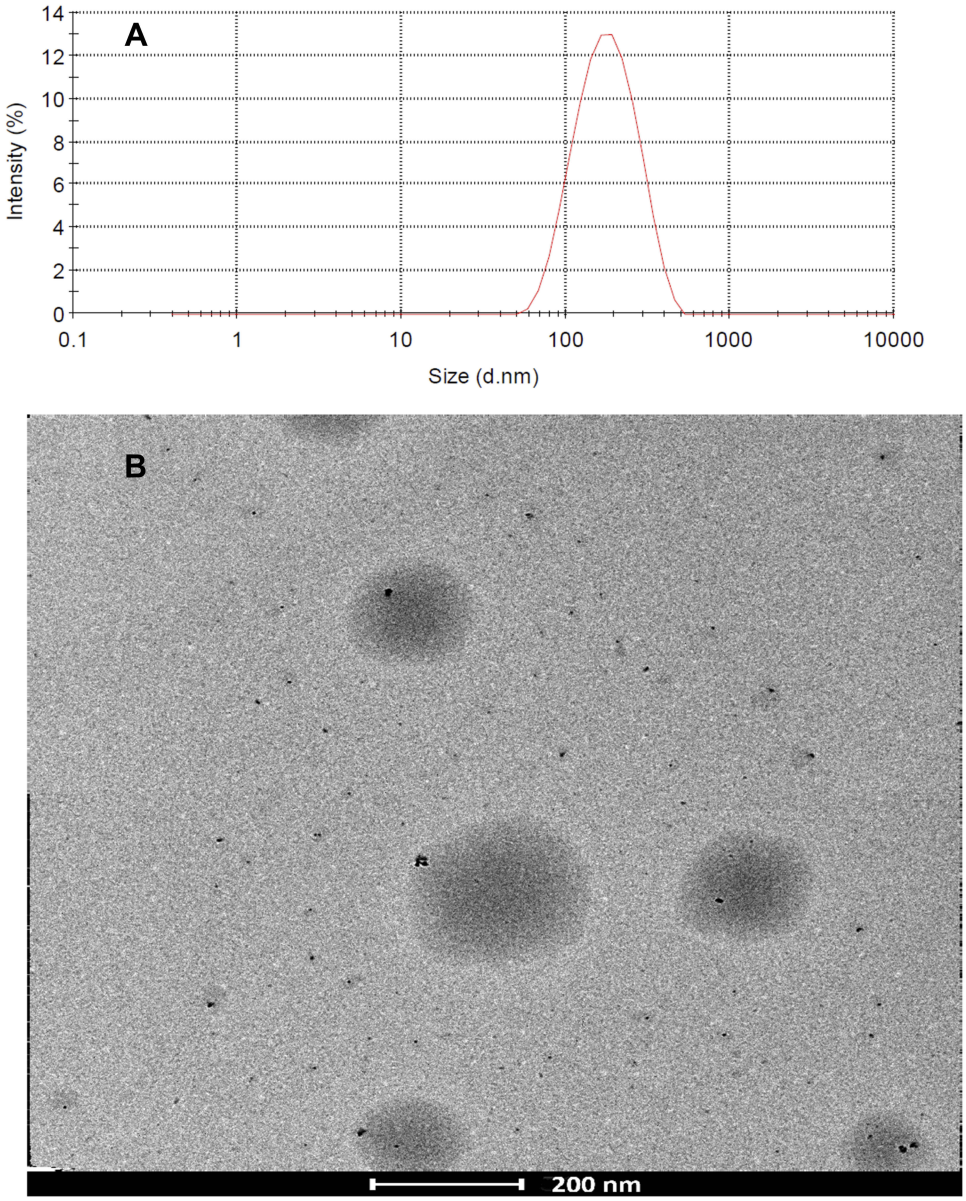

Figure 7 The DLS and TEM image of urushiol-loaded polymeric micelles.
Notes: (**A**) Size distribution. (**B**) TEM image.
Abbreviations: DLS, dynamic light scattering; TEM, transmission electron microscopy.

they undergo significant decomposition in response to acidic conditions, such as those found within endosomes.

Blood has a pH of 7.4; as such, micelles should remain stable in this solution, whereas the pH falls to 5.5–6.0 in endosomes and 4.5–5.0 in lysosomes. Thus, pH-sensitive micelles will only release their cargo in cells, thus reducing off-target toxicity and increasing intratumoral drug accumulation.[21] We therefore studied the kinetics of urushiol release from micelles in solutions with different pH values (5.0, 6.5, 7.4) in an effort to simulate extracellular and endolysosomal environments. We found that urushiol release was pH-dependent, with this drug being released more rapidly under low pH conditions. At a pH of 7.4, only 23.54% of urushiol was released from these micelles within 72 h (Figure 9B), whereas, at a pH of 6.5, urushiol release was 58.60% at 24 h and 61.65% at 72 h. At a lower pH of 5.0, 20.42% of urushiol was released within 2 h, with release rates rising to 91.52% at 10 h and 98.74% at 72 h. This more rapid release of urushiol under acidic conditions is likely attributable to the same mechanisms responsible for the decreased stability of polymeric micelles under these same conditions. Our findings thus confirm that urushiol-loaded micelles are

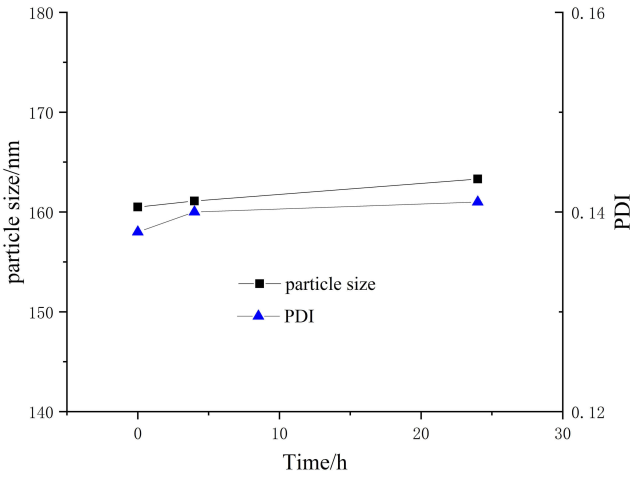

Figure 8 The particle size and PDI change of urushiol-loaded polymeric micelles in FBS within 24 hours. Error bars represent the standard deviation (n = 3).
Abbreviations: PDI, polydispersity index; FBS, fetal bovine serum.

likely to be stable at a normal physiological pH, whereas they are able to rapidly release urushiol within the endolysosome following endocytosis.

In vitro Cytotoxicity Assay

We next sought to explore the cytotoxic efficacy of our urushiol-loaded micelles in vitro using MCF-7 breast cancer cells in an MTT viability assay. We found that blank micelles did not induce significant tumor cell toxicity even at high concentrations (500 mg/mL), indicating that the copolymer exhibits an excellent safety and biocompatibility profile (Figure 10A). In contrast, MCF-7 cell growth was significantly impaired when cells were treated with free or micelle-encapsulated urushiol in a dose-dependent manner (Figure 10B). Importantly, at concentrations between 0.001 and 20 mg/L, urushiol-loaded micelles exhibited superior cytotoxicity relative to free urushiol ($P < 0.01$). Free urushiol and urushiol-loaded micelles were found to have respective IC_{50} values of 3.42 mg/L and 1.21 mg/L. We thus found that urushiol-loaded micelles were more cytotoxic than urushiol, likely because the amphiphilic polymers that compose these micelles function similarly to surfactants, increasing membrane mobility and micelle diffusion into these tumor cells. After these micelles are taken into cells, they dissociate when exposed to acidic lysosomal conditions, thus allowing urushiol to accumulate intracellularly. In addition, polymer micelles may prevent drug efflux from the P-glycoprotein (P-gp) pump by inhibiting P-gp expression, thus increasing the intracellular drug concentration and enhancing antitumor activity.[27–30]

Pharmacokinetic Analyses

We utilized a noncompartmental model to analyze the pharmacokinetics of free urushiol and urushiol-loaded polymeric micelles following their intravenous administration in rats. The resultant pharmacokinetic parameters are compiled in Table 7. We found that the pharmacokinetic properties of urushiol-loaded micelles differed significantly from those of free urushiol (Figure 11). Peak plasma concentrations (C_{max}) of 10.5 mg/L or 8.08 mg/L were achieved following urushiol-loaded micelle or free urushiol administration, respectively. These urushiol-loaded micelles had significantly higher total area-under-the-curve (AUC) and mean residence time (MRT) values relative to free urushiol (2.28- and 2.53-fold increases,

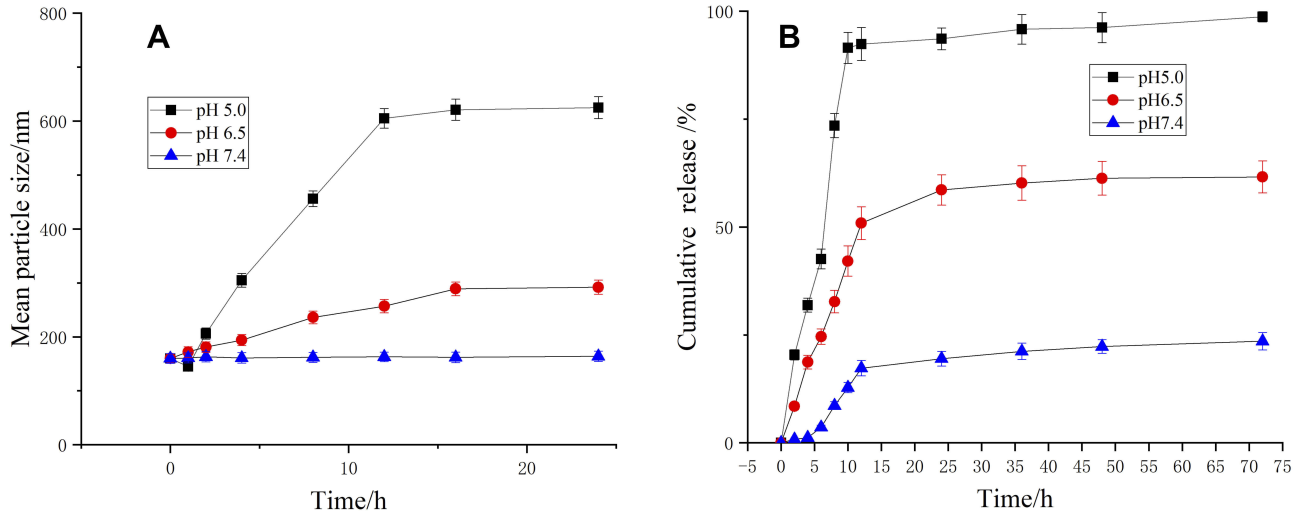

Figure 9 (**A**) The particle size change of urushiol-loaded polymeric micelles at various pH values; (**B**) in vitro urushiol release kinetics from urushiol-loaded polymeric micelles under different pH values. Error bars represent the standard deviation (n = 3).

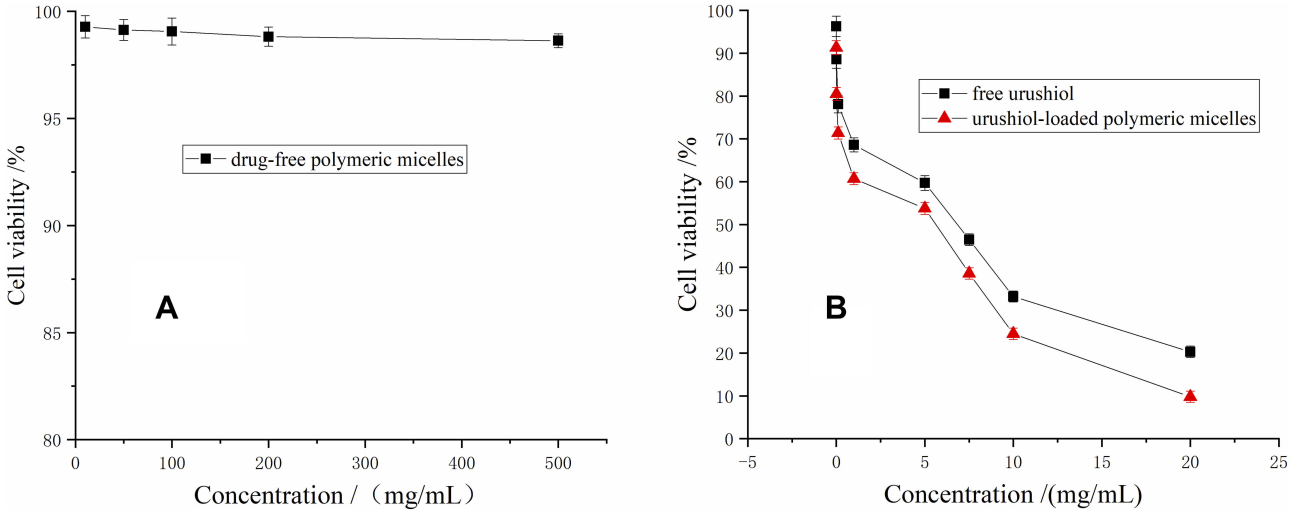

Figure 10 In vitro cytotoxicity of drug-free polymeric micelles (**A**), free urushiol (**B**) and urushiol-loaded micelles (**B**) at different concentrations in MCF-7 cells. Error bars represent the standard deviation (n = 3).

respectively). This suggests that these drug-loaded micelles were able to remain in circulation for longer than free urushiol. We further found that urushiol encapsulation was associated with a reduction in body clearance (CL) from 0.77 to 0.23 L/h/kg, with $t_{1/2}$ being significantly increased from 1.10 to 8.00 h relative to free urushiol. This suggests that the micellar encapsulation of urushiol prevents its clearance in vivo, thus extending its circulation time. Chemical conjugation in these micelles may have also improved their stability, thereby facilitating prolonged and sustained drug release in vivo.

Analysis of the in vivo Antitumor Efficacy of Urushiol-Loaded Micelles

Lastly, we sought to evaluate the ability of our drug-loaded micelles to treat tumors in vivo in Kunming mice bearing MCF-7 xenograft tumors. We found that control mice administered normal saline (NS) exhibited rapid tumor growth, whereas tumor growth was slowed in response to urushiol administration (Figure 12A). Importantly, urushiol-loaded micelles exhibited more significant tumor growth inhibition relative to free urushiol (72.47% vs 53.85%). The reduced efficacy of free urushiol may be associated with its more rapid clearance and lower rates of accumulation in organs relative to encapsulated urushiol. These findings clearly demonstrated the improved therapeutic efficacy of urushiol-loaded polymeric micelles, as they improved urushiol delivery to the tumors owing to the de-micellization that occurred

Table 7 Pharmacokinetic Parameters of the Free Urushiol and Urushiol-Loaded Polymeric Micelles

Parameters	Free Urushiol	Urushiol-Loaded Polymeric Micelles
C_{max} (mg/L)	8.08 ±1.12	10.5±1.37
AUC (mg h/L)	25.75 ±2.56	84.48 ± 4.62*
AUMC (mg h^2/L)	75.10 ± 4.01	859.45 ± 8.64**
$t_{1/2}$ (h)	1.10 ±0.02	8.00 ± 1.05*
MRT (h)	2.88 ± 0.13	10.17 ±1.96 *
CL (L/h/kg)	0.77 ±0.11	0.23 ± 0.01*
V (L/kg)	1.23 ± 0.05	2.69 ± 0.34

Notes: Data presented as mean ± standard deviation (n=3). *p < 0.05 and **p < 0.01.

Abbreviations: C_{max}, peak plasma concentrations; AUC, total area-under-the-curve; AUMC, area under the first moment curve; $t_{1/2}$, half-life period; MRT, mean residence time; CL, body clearance; V, volume.

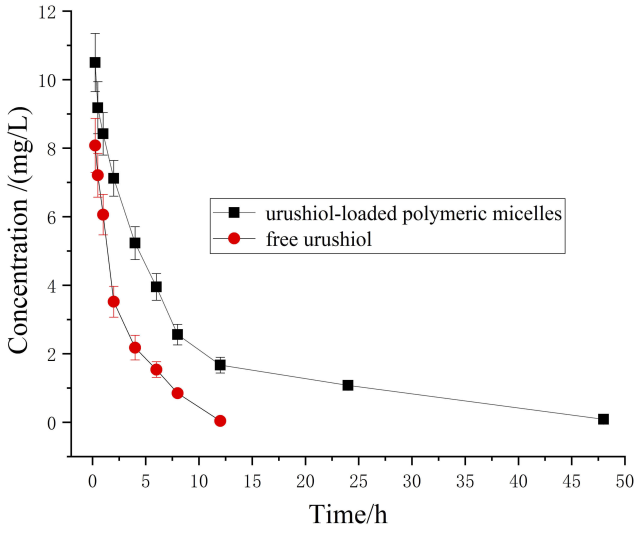

Figure 11 Plasma concentration-time profiles of urushiol after intravenous injection of free urushiol and urushiol-loaded micelles in rats. Error bars represent the standard deviation (n = 3).

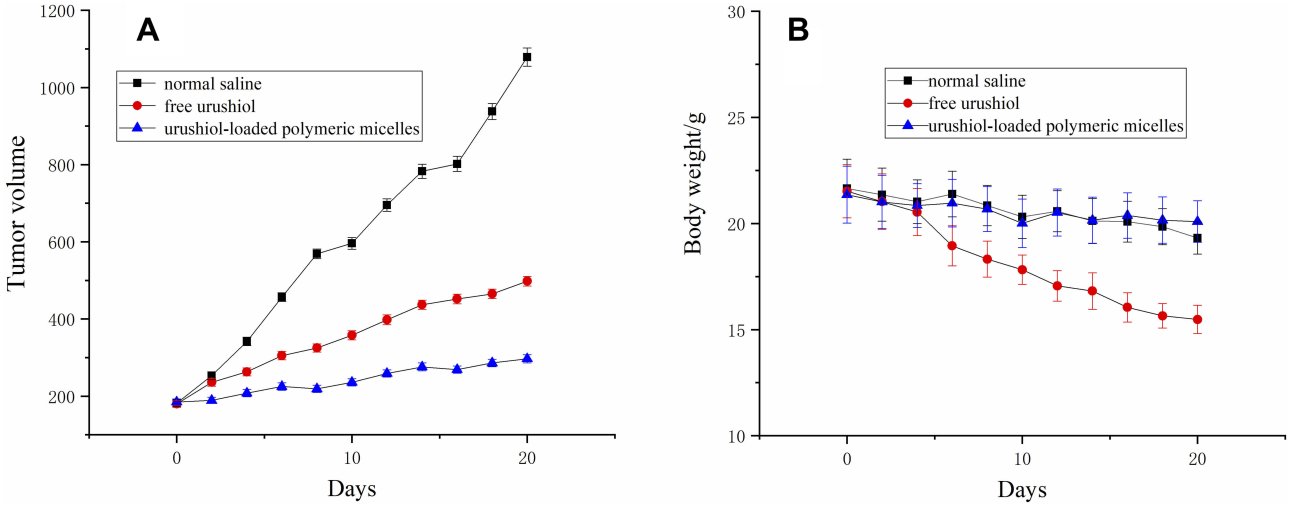

Figure 12 In vivo therapeutic efficacy of urushiol-loaded micelles. (**A**) The mean tumor volume changes and (**B**) body weight changes of tumor-bearing mice treated with saline, free urushiol and urushiol-loaded micelles. Error bars represent the standard deviation (n = 3).

only in acidic intracellular or intratumoral environments.[31] We additionally monitored the body weight of treated mice to assess the off-target toxicity of tested treatments. We observed a significant decline in the body weight of mice administered free urushiol, suggesting that it caused substantial nonspecific toxicity following intravenous delivery (Figure 12B). In contrast, mice administered urushiol-loaded polymeric micelles did not significantly lose weight during the study period, suggesting that encapsulation can significantly mitigate urushiol-associated toxicity.

We measured the levels of urushiol within different tissues at the indicated study time points to understand the drug tissue distribution profiles associated with our polymeric micelles (Tables 8 and 9). We found that free or encapsulated urushiol administration was followed by the rapid distribution of urushiol in tissues, including the liver, spleen, kidneys, lungs, and heart, with this drug thereafter being eliminated in a time-dependent fashion. In contrast, maximal concentrations of urushiol were achieved at a later time point (~2 h post-administration), and drug elimination from these tissues was more gradual. Consistent with our above observations, intratumoral urushiol concentrations were significantly higher within 12 h of drug administration when animals were administered urushiol-loaded micelles compared to free urushiol, suggesting that these particles achieved superior tumor targeting. This may be a consequence of the hypervascular permeability and impaired lymphatic drainage that characterize tumors, thus leading to increased micelle accumulation.[32] The pH-sensitive nature of these micelles can further increase intratumoral urushiol accumulation. The higher amounts of urushiol detected in the kidneys of treated mice suggest that these micelles are subject to renal elimination. As cardiac urushiol levels were lower in these treated mice, this

Table 8 Tissue Distribution of Urushiol Determined in Tumor-Bearing Mice After i.v. Administration of Urushiol-Loaded Polymeric Micelles

Time (h)	Liver (μg/g)	Spleen (μg/g)	Kidneys (μg/g)	Lungs (μg/g)	Heart (μg/g)	Tumor (μg/g)
0.083	51.4 ± 4.41	10.3 ± 1.05	37.4 ± 3.03	16.9 ± 1.85	11.6 ± 1.15	60.8 ±4.32
0.5	29.3 ± 2.63	7.73 ± 1.25	28.6 ±2.83	15.0 ± 1.26	7.14 ± 1.06	66.5 ± 5.01
1	25.2 ± 2.34	6.86 ± 0.97	29.5 ± 3.12	10.8 ±1.22	6.32 ± 1.03	84.3 ± 5.89
2	21.6 ± 2.06	5.25 ± 0.47	14.7 ± 1.73	7.69 ±1.08	3.68 ± 0.65	92.4 ± 6.24
4	11.5 ± 1.03	3.03 ± 0.28	10.8 ± 1.14	5.26 ± 1.01	2.72 ± 0.48	74.3 ± 5.18
8	5.34 ± 0.69	2.06 ± 0.12	8.33 ± 1.12	2.17 ± 0.24	1.32 ± 0.42	58.6 ± 4.04
12	1.13 ± 0.25	NQ	1.52 ± 0.56	NQ	NQ	46.9 ± 3.17

Notes: Data represent mean value ± SD for three mice. NQ: not quantified.
Abbreviation: i.v., intravenously.

Table 9 Tissue Distribution of Urushiol Determined in Tumor-Bearing Mice After i.v. Administration of Free Urushiol

Time (h)	Liver (μg/g)	Spleen (μg/g)	Kidneys (μg/g)	Lungs (μg/g)	Heart (μg/g)	Tumor (μg/g)
0.083	47.2 ± 3.69	13.3 ± 1.65	22.3 ± 2.63	28.3 ± 2.78	29.5±2.93	35.2± 3.29
0.5	30.4 ± 3.17	11.6 ± 1.45	30.5 ± 3.06	20.5 ±2.32	20.8 ± 2.05	48.2 ± 4.01
1	31.2± 3.11	10.5 ± 1.39	15.7 ± 1.45	12.4 ± 1.85	12.7 ± 1.68	43.3± 3.59
2	22.8± 2.65	8.46 ± 0.78	11.6± 1.14	10.9 ± 1.34	8.13 ± 1.02	49.2± 3.63
4	17.5± 2.23	6.28 ± 0.65	7.23 ± 1.62	7.69 ± 1.05	5.93 ± 0.87	38.8±3.13
8	10.56 ± 1.65	5.85 ± 0.74	4.25 ± 1.02	4.35 ± 0.87	4.04 ± 0.32	31.5 ± 2.57
12	2.87 ± 0.68	2.07 ± 0.13	1.32 ± 0.39	NQ	1.81 ± 0.15	18.4 ± 1.34

Notes: Data represent mean value ± SD for three mice. NQ: not quantified.
Abbreviation: i.v., intravenously.

also suggests that urushiol encapsulation may lower associated rates of cardiac toxicity. Together, these findings suggest that urushiol encapsulation can significantly increase intratumoral drug concentrations, thus improving the therapeutic efficiency of this drug.

Conclusions

In the present study, we developed mPEG-PBAE copolymer-based micelles that could be readily used to encapsulate urushiol for delivery to tumor tissues. We initially synthesized four different mPEG-PBAE copolymers using different mPEG-NH_2 or hydrophobic amino types, and then characterized these particles based upon GPC, CMC, and other analyses. This led us to ultimately select the $mPEG_{5000}$-PBAE-C_{12} polymer, which was then used for urushiol encapsulation using a dialysis-based strategy. We optimized our micelle formulation strategy via an RSM approach, leading us to successfully prepare small urushiol-loaded polymeric micelles that had high drug loading and encapsulation efficiencies. These particles were pH-sensitive, such that they were highly stable at a normal physiological pH, whereas they readily released urushiol when exposed to acidic conditions. These micelles were further found to effectively impair MCF-7 tumor cell proliferation in vitro, disrupting the growth of these cells more effectively than free urushiol. In a murine xenograft model system, we additionally determined that these urushiol-loaded micelles were readily able to impair MCF-7 tumor growth. These particles also had enhanced pharmacokinetics, including a prolonged circulation time and an increased intratumoral drug accumulation relative to free urushiol. Together, these results indicate that urushiol-loaded polymeric micelles can significantly improve the solubility of urushiol while lowering its off-target toxicity and enhancing its antitumor activity, emphasizing the importance of further studying the clinical utility of these particles in future studies.

Ethical and Legal Approval

All protocols followed in the animal experiments were approved by the Animal Ethics Committee of Nanjing Medical University, and in accordance with the principles of "Guide for the Care and Use of Laboratory Animals" and "The Guidance to Experimental Animal Welfare and Ethical Treatment" established by the National Science Council of the Republic of China. All efforts were made to minimize animal suffering.

Acknowledgments

The authors are grateful for the financial support from the National Natural Science Foundation of China (31600467).

Disclosure

The authors report no conflicts of interest in this work.

References

1. Siegel RL, Miller KD, Jemal A. Cancer statistics. *CA Cancer J Clin*. 2016;66(1):7–30. doi:10.3322/caac.21332
2. Yakun M, Fan XH, Li LB. pH-sensitive polymeric micelles formed by doxorubicin conjugated prodrugs for co-delivery of doxorubicin and paclitaxel. *Carbohydr Polym*. 2016;137:19–29. doi:10.1016/j.carbpol.2015.10.050
3. Ye FY, Lei DD, Wang SM, Zhao GH. Polymeric micelles of octenyl-succinated corn dextrin as vehicles to solubilize curcumin. *LWT*. 2017;75:187–194.
4. Naksuriya O, Shi Y, Van Nostrum CF, Anuchapreeda S, Hennink WE, Okonogi S. HPMA-based polymeric micelles for curcumin solubilization and inhibition of cancer cell growth. *Eur J Pharm Biopharm*. 2015;94:501–512.
5. Maeda H. Tumor-selective delivery of macromolecular drugs via the EPR effect: background and future prospects. *Bioconjugate Chem*. 2010;21:797–802.
6. Torchilin VP. Structure and design of polymeric surfactant-based drug delivery systems. *J. Control Release*. 2001;73(2–3):137–172. doi:10.1016/s0168-3659(01)00299-1
7. Cabral H, Kataoka K. Progress of drug-loaded polymeric micelles into clinical studies. *J Control Release*. 2014;190:465–476.

8. Yang HY, Jang MS, Gao GH, Lee JH, Lee DS. Construction of redox/pH dual stimuli-responsive PEGylated polymeric micelles for intracellular doxorubicin delivery in liver cancer. *Polym Chem*. 2016;7:1813–1825.
9. Demirdirek B, Uhrich KE. Salicylic acid-based pH-sensitive hydrogels as potential oral insulin delivery systems. *J Drug Target*. 2015;23(7–8):716–724. doi:10.3109/1061186X.2015.1073293
10. Estrella V, Chen T, Lloyd M, et al. Acidity generated by the tumor microenvironment drives local invasion. *Cancer Res*. 2013;73(5):1524–1535. doi:10.1158/0008-5472.CAN-12-2796
11. Xu ZG, Xue P, Gao YE, et al. pH-responsive polymeric micelles based on poly (ethyleneglycol)-b-poly (2-(diisopropylamino) ethyl methacrylate) block copolymer for enhanced intracellular release of anticancer drugs. *J Colloid Interf Sci*. 2017;490:511–519. doi:10.1016/j.jcis.2016.11.091
12. Chen W, Zhong P, Meng FH, et al. Redox and pH-responsive degradable micelles for dually activated intracellular anticancer drug release. *J Control Release*. 2013;169(3):171–179. doi:10.1016/j.jconrel.2013.01.001
13. Xue YN, Huang ZZ, Zhang JT, et al. Synthesis and self-assembly of amphiphilic poly (acrylic acid-b-DL-lactide) to form micelles for pH-responsive drug delivery. *Polymer*. 2009;50(15):3706–3713. doi:10.1016/j.polymer.2009.05.033
14. Honda T, Lu R, Sakai R, Ishimura T, Miyakoshi T. Characterization and comparison of Asian lacquer saps. *Prog Org Coat*. 2008;61(1):68–75. doi:10.1016/j.porgcoat.2007.09.003
15. Hong DH, Han SB, Lee CW, et al. Cytotoxicity of urushiols isolated from sap of Korean lacquer tree (Rhus vernicifera Stokes). *Arch Pharm Res*. 1999;22(6):638–641. doi:10.1007/BF02975339
16. Wang CZ, He YF, Zhou H, et al. Preparation and characterization of urushiol methylene acetal derivatives with various degrees of unsaturation in alkyl side chain. *Int J Polym Sci*. 2015;3:1–6.
17. Mozhi A, Ahmad I, Okeke CI, Li C, Liang XJ. pH-sensitive polymeric micelles for the Co-delivery of proapoptotic peptide and anticancer drug for synergistic cancer therapy. *RSC Adv*. 2017;7(21):12886–12896. doi:10.1039/C6RA27054A
18. Woraphatphadung T, Sajomsang W, Gonil P, et al. pH-Responsive polymeric micelles based on amphiphilic chitosan derivatives: effect of hydrophobic cores on oral meloxicam delivery. *In. J Pharmaceut*. 2016;497(1–2):150–160. doi:10.1016/j.ijpharm.2015.12.009
19. Mehanny M, Hathout RM, Geneidi AS, Mansour S. Bisdemethoxycurcumin loaded polymeric mixed micelles as potential anti-cancer remedy: preparation, optimization and cytotoxic evaluation in a HepG-2 cell model. *J Mol Liq*. 2016;214:162–170. doi:10.1016/j.molliq.2015.12.007
20. Le Garrec D, Gori S, Luo L, et al. Poly (N-vinylpyrrolidone)-block-poly (D, L-lactide) as a new polymeric solubilizer for hydrophobic anticancer drugs: in vitro and in vivo evaluation. *J. Control Release*. 2004;99(1):83–101. doi:10.1016/j.jconrel.2004.06.018
21. Zhang JL, Zhao XF, Chen Q, et al. Systematic evaluation of multifunctional paclitaxel-loaded polymeric mixed micelles as a potential anticancer remedy to overcome multidrug resistance. *Acta Biomater*. 2017;50:381–395. doi:10.1016/j.actbio.2016.12.021
22. Zhao Y, Zhou YX, Wang DS, et al. pH-responsive polymeric micelles based on poly (2-ethyl-2-oxazoline)-poly (D, L-lactide) for tumor-targeting and controlled delivery of doxorubicin and P-glycoprotein inhibitor. *Acta Biomater*. 2015;17:182–192. doi:10.1016/j.actbio.2015.01.010
23. Zeng C, Jiang W, Tan ME, et al. Optimization of the process variables of tilianin-loaded composite phospholipid liposomes based on response surface-central composite design and pharmacokinetic study. *Eur J Pharm Sci*. 2016;85:123–131. doi:10.1016/j.ejps.2016.02.007
24. Chu BY, Shi S, Li XY, et al. Preparation and evaluation of teniposide-loaded polymeric micelles for breast cancer therapy. *Int J Pharm*. 2016;513(1–2):118–129. doi:10.1016/j.ijpharm.2016.09.005
25. Vermette P, Meagher L. Interactions of phospholipid- and poly(ethylene glycol)-modified surfaces with biological systems: relation to physico-chemical properties and mechanisms. *Colloid Surf B*. 2003;28(2):153–198. doi:10.1016/S0927-7765(02)00160-1
26. Wang LL, Zhang J, Song MJ, et al. shell-crosslinked polymeric micelle system for pH/redox dual stimuli-triggered DOX on-demand release and enhanced antitumor activity. *Colloid Surf B*. 2017;152:1–11. doi:10.1016/j.colsurfb.2016.12.032
27. Su ZH, Liang YC, Yao Y, Wang TQ, Zhang N. Polymeric complex micelles based on the double-hydrazone linkage and dual drug-loading strategy for pH-sensitive docetaxel delivery. *J Mater Chem B*. 2016;4(6):1122–1133. doi:10.1039/c5tb02188j
28. Li NN, Zhang P, Huang CZ, Song YM, Garg S, Luan YX. Co-delivery of doxorubicin hydrochloride and verapamil hydrochloride by pH-sensitive polymersomes for the reversal of multidrug resistance. *RSC Adv*. 2015;5(95):77986–77995. doi:10.1039/C5RA15313A
29. Yi XQ, Zhang Q, Zhao D, et al. Preparation of pH and redox dual-sensitive core crosslinked micelles for overcoming drug resistance of DOX. *Polym Chem*. 2016;7:1719–1729.
30. Zhang L, Lu JF, Jin YM, Qiu LY. Folate-conjugated beta-cyclodextrin-based polymeric micelles with enhanced doxorubicin antitumor efficacy. *Colloid Surf B*. 2014;122:260–269.
31. Bui QN, Li Y, Jang MS, Huynh DP, Lee JH, Lee DS. Redox-and pH-sensitive polymeric micelles based on poly (β-amino ester)-grafted disulfide methylene oxide poly (ethylene glycol) for anticancer drug delivery. *Macromolecules*. 2015;48(12):4046–4054. doi:10.1021/acs.macromol.5b00423
32. Emami J, Rezazadeh M, Hasanzadeh F, et al. Development and in vitro/in vivo evaluation of a novel targeted polymeric micelle for delivery of paclitaxel. *Int J Biol Macromol*. 2015;80:29–40. doi:10.1016/j.ijbiomac.2015.05.062